W-band Electronic Focus-Scanning by a Reconfigurable Transmitarray for Millimeter-Wave Imaging Applications

Xiaotian Pan, Fan Yang, Shenheng Xu, and Maokun Li

Department of Electrical Engineering
Tsinghua University, Beijing, 100084, China
fan_yang@tsinghua.edu.cn

Abstract ─ A w-band electronic focus-scanning function, which is desired for high-resolution fast-speed millimeter-wave imaging systems, is realized by a reconfigurable transmitarray antenna (RTA). As a two-layer structure, each RTA element is integrated with two packaged PIN diodes symmetrically within a limited area ($1.6\times1.6mm^2$). When a linearly polarized electromagnetic wave incidents on this reconfigurable element, an orthogonally polarized transmission wave is generated, with the ability of 1-bit phase adjustment (0°/180°). Using this element, a 32×2 reconfigurable transmitarray is designed and fabricated to realize 1-D steerable focal points in a near-distance focal plane. The measured focal points agree well with the design, illustrating the feasibility of the proposed RTA for w-band microwave imaging systems.

Index Terms ─ Antennas, PIN diode, reconfigurable, transmitarray, W-band.

I. INTRODUCTION

W-band microwave imaging systems have advantages of good penetrability and high resolution, especially suitable for applications of security checking [1]. For this type of near-distance imaging applications, the image resolution and scanning rate are two important objectives. As a core component, a high-performance low-cost w-band electronically-scanning antenna remains challenging [2].

By integrating electrically tunable components into transmitarray element, steerable beams are realized by RTAs [3]. The low-cost and low-profile features of RTAs make these antennas promising alternatives for conventional phased arrays. At w band, liquid crystal (LC) and micro electro mechanical system (MEMS) have been applied in reconfigurable antennas [4-5]. However, the switching time, material loss, and complicated fabrication process are still concerns. Meanwhile, PIN diode [6], as a common electrical component, has been applied for RTAs in Ka band [7-8], and shows promising potential in higher frequency band. Furthermore, the switching time at nanosecond level of PIN diode guarantees fast beam-switching speed, especially suitable for high-speed imaging applications.

In this work, a 1-D PIN-controlled RTA is designed for focus scanning at 96.5GHz. A two-layer RTA element with switchable resonance structure integrated with two packaged PIN diodes is proposed to realize a 180° phase shift. This symmetrical structure can generate an orthogonally polarized transmission wave with 1-bit phase shift precisely, overcoming the adverse effects from uncertain parasitic parameters of PIN diode and fabrication error of PCB at such high frequency band. A 32×2 RTA prototype has been fabricated for steerable focal points at near distance. Measured focal points match well with calculated results. This antenna shows a low-cost solution for microwave imaging systems with high-resolution and high scanning rate.

II. ANTENNA DESCRIPTION

The antenna consists of three parts: an open-end waveguide (WR10), a parallel-plate waveguide, and a 1-D arrays of two-row RTA elements, as shown in Fig. 1. The waveguides support an incident y-polarization wave. Each element receives the incident wave, changes the phase, and then radiates for the x-polarized scanning focuses. The phase of the transmitted wave can be adjusted to be 0° or 180° electronically by the RTA. The element design and the phase distribution for the focus scanning are presented in this section in detail.

A. Element design and working principle

Traditional RTA elements usually have three or more layers to achieve enough reconfigurability of transmission phase [7]. However, these designs require accurate alignment during assembling layers, which is challenging at w band. To solve this problem, a novel RTA element is designed as a two-layer structure that can be directly printed on opposite sides of one substrate, as shown in Fig. 2. Being a coupling layer, the first layer of the element is a rectangular slot. This layer couples a y-polarized incident electromagnetic wave to a U-shaped

Submitted On: January 6, 2020
Accepted On: March 16, 2020

microstrip resonance structure on the second layer. Two PIN diodes are integrated on the U-shaped microstrip line for reconfigurability.

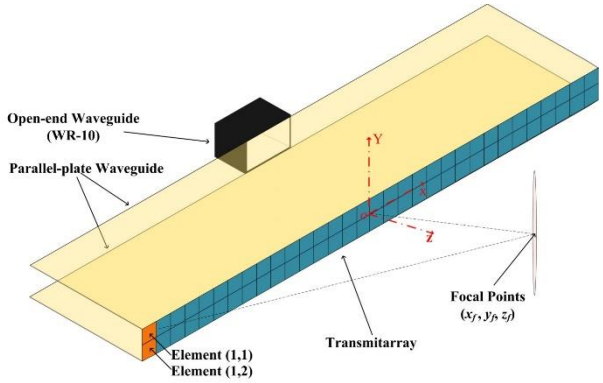

Fig. 1. W-band transmitarray design with 1-D steerable focal points.

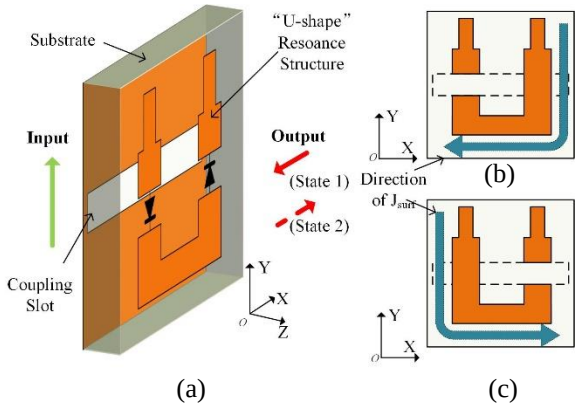

Fig. 2. Schematic and operation principle of the RTA element: (a) Geometry of element; (b) Ideal case 1; (c) Ideal case 2.

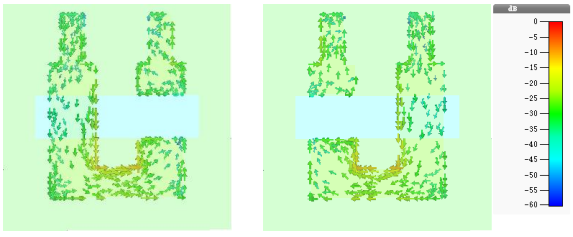

Fig. 3. Current distributions on the ideal element under two states: (a) State 1 and (b) State 2.

At state 1, the left PIN diode is at "ON" condition, and the right one is at "OFF" condition. For state 2, working conditions of two PIN diodes are opposite to state 1. Under different states of PIN diodes, one side of the U-shaped structure is cut off. Two ideal cases can be used to illustrate working principle of the RTA element. Current distributions of the element under two states are shown as Fig. 3. Two symmetrical L-shaped resonance structures are formed, and generate symmetrically surface current J_{surf} on the resonators. The element will produce output waves with both y-polarization and x-polarization. It is worthy to mention that, when the states of PIN diodes change, the y-polarized wave remains the same, but the x-polarized wave has an 180° phase difference due to the opposite current direction as shown before. Hence, the x-polarized wave with the phase tuning capability is used for focusing and scanning in this paper, and the y-polarized wave cannot. The transmission coefficients T_{xy} for the x-polarized output wave under two cases follow the equation as below:

$$\arg(T_{xy})|_{\text{State 2}} - \arg(T_{xy})|_{\text{State 1}} = \pi. \quad (1)$$

B. Element simulation and optimization

The element is designed on Rogers 5880 dielectric substrate with the thickness of h_p=0.508mm, ε_r=2.2 and tanδ=0.0009. The period of the element is p_c=1.6 mm. A mm-wave PIN diode (MA4AGFCP910) is chosen as the w-band switch component because of its highest cut-off frequency compared with other commercially available PIN diodes [9]. The bias structure is designed for supplying controlling voltages for these PIN diodes, as shown in Fig. 4. Electromagnetic simulation software CST is used to analyze these elements by setting periodic boundary conditions. Series RLC model is used to describe the RF impedance characteristic of PIN diode [10]. In CST, the series RLC model of PIN diode is set according to the online datasheet: R_{on}=4Ω, L_{on}=10pH; R_{off}=3Ω, L_{off}=10pH, C_{off}=18fF.

In order to acquire the optimum magnitude of T_{xy} at working frequency, parameters of the element are studied through EM simulations. For the receiving layer, the working frequency decreases with the increasing length of s_x, which mainly affects the working mode of the slot, as shown in Fig. 5. For the second layer, the effective current path of the working mode increases with the lengths of both the x-direction part and the y-direction part in the L-shaped resonance structures. As a result, the working frequency is expected to decrease with larger sizes: g_x, b_u, as shown in Figs. 6 & 7. Other parameters of the L-shaped structure are defined by the standard sizes of soldering pad for the PIN diode [9]. After optimizing these antenna parameters through EM simulations, a practical 1-bit RTA at w band is achieved. Detailed sizes of the RTA element are shown in the caption of Fig. 4, as well as the biasing structure.

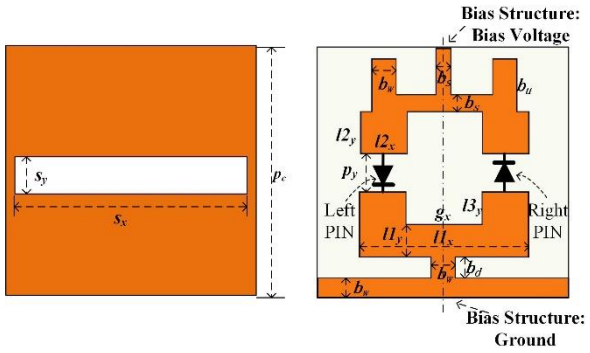

Fig. 4. Detailed sizes of RTA element with a bias structure: (a) first layer of the reconfigurable element; (b) second layer of the reconfigurable element. (s_x=1.15, s_y=0.3, b_w=0.15, b_u=0.35, b_s=0.1, p_y=0.33, b_w=0.15, b_d=0.135, b_x=0.185, $l1_x$=0.93, $l1_y$=0.2, $l2_x$=0.31, $l2_y$=0.2, $l3_y$=0.2, g_x=0.31. Unit: mm).

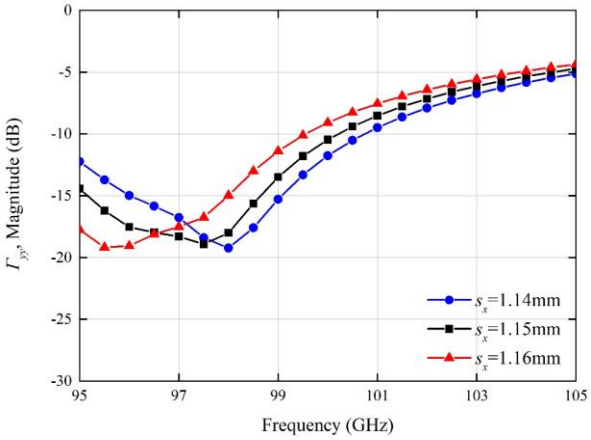

Fig. 5. Magnitude of Γ_{yy} versus different values of s_x.

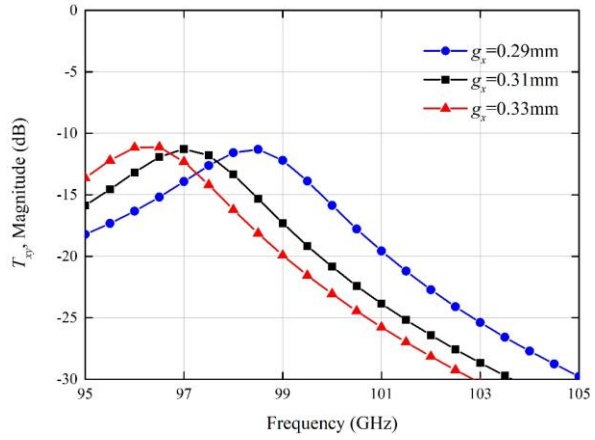

Fig. 6. Magnitude of T_{xy} versus different values of g_x.

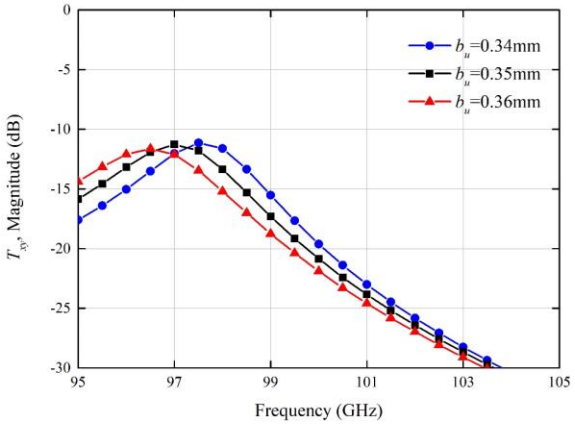

Fig. 7. Magnitude of T_{xy} versus different values of b_u.

The transmission phases of the ideal case and the practical PIN case are different due to the practical diode model and the existence of the biasing circuit. However, the phase difference between states 1 & 2 remains to be 180° due to the symmetrical element design, as shown in Figs. 8 & 9. Hence, the proposed element can guarantee the precise 180° phase shift, regardless of the PIN model and the biasing effect.

In contrast, the magnitude of transmission coefficient T_{xy} of the RTA element is dependent on the PIN model. For the ideal case, the maximum of T_{xy} is -3.1dB at 101.5GHz, as shown in Fig. 10. Meanwhile, the corresponding T_{yy} value is -3.5dB, which shows that the proposed element converts more energy into the cross-polarized wave than that in the co-polarized wave. For the practical PIN model, the maximum of T_{xy} is -11.1dB at 97GHz. The distinct difference between the two models is the value of C_{off}, which controls the polarization conversion efficiency (T_{xy}) of the antenna. To study influence of the capacitance C_{off}, different reconfigurable elements with the increasing value of capacitance C_{off}, have been simulated. Magnitudes of the simulated transmission coefficients of RTA element, are shown in Fig. 11. As a result, with the value of C_{off} decreasing, magnitude of the transmission coefficient T_{xy} increases, leading to a better element performance.

Another reason is the biasing circuit effect. In the ideal design, high-impedance microstrip lines with large resistance value are needed to reduce the influence of outer biasing structure [11]. However, limited by the PCB fabrication technology (minimum width of the bias line is 0.1mm), the width of the biasing line is close to that of the resonance structure, and does affect the performance of the RTA element. After adding the biasing structure, the new shape is more like a split-ring resonator. The parameters are optimized to get an acceptable polarization conversion efficiency.

In summary, the proposed RTA element has a relatively large insertion loss due to the limitations of available PIN diode (large C_{off} value) and fabrication process (0.1 mm line width). However, it is worth noting that precise 1-bit phase shift can be guaranteed even under these two adverse effects, which is critical for high-resolution applications.

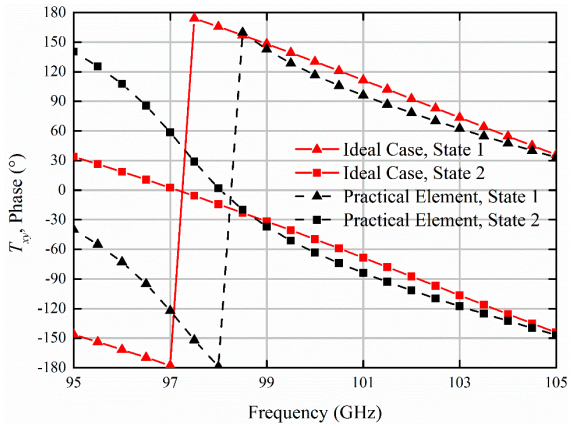

Fig. 8. Simulated results of T_{xy} phase under different element models.

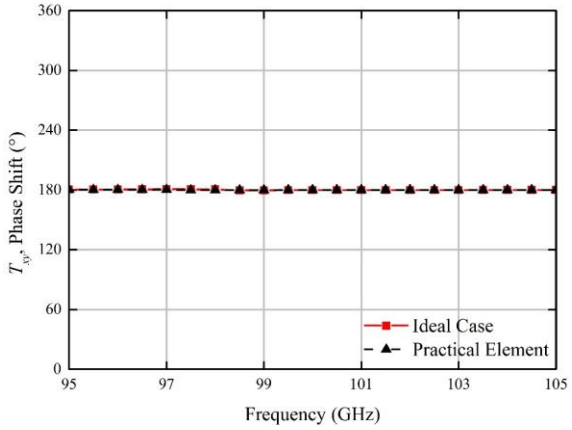

Fig. 9. Simulated results of phase shift under different element models.

C. Transmitarray with 1-D steerable focal points

1-D steerable focal points on a focal plane can be used for near-field imaging system. A 32×2 reconfigurable transmitarray antenna (RTA) is designed for this purpose. An open-end waveguide generates the electromagnetic wave of TE_{10} mode and radiates it to the RTA located at the end of a parallel-plate waveguide, as shown in Fig. 1. The length of the parallel-plate waveguide along z-direction is 27.5mm. Incident phase distribution and magnitude distribution on the RTA aperture are measured. The measured illumination taper at the edge of the array is -11.9dB.

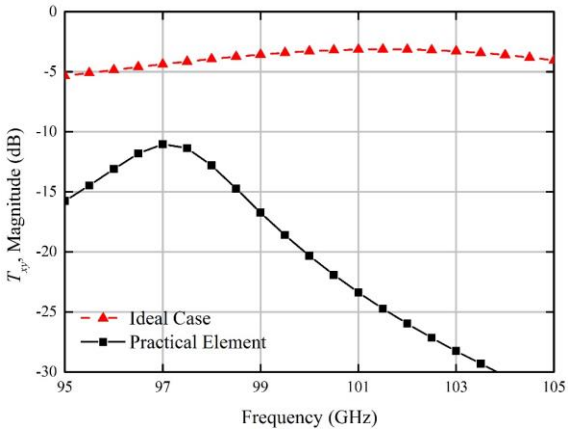

Fig. 10. Simulated results of T_{xy} magnitude under different element models.

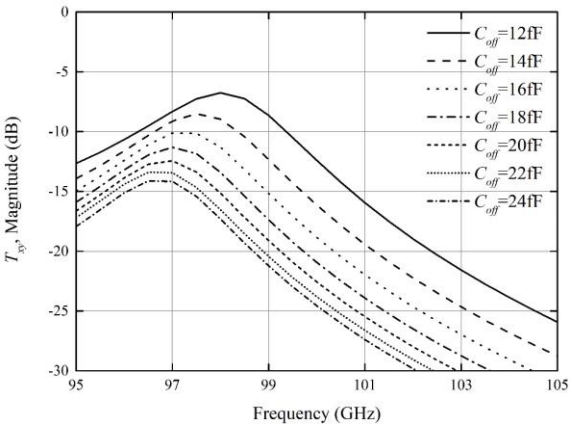

Fig. 11. Magnitude of T_{xy} versus different values of capacitances C_{off}. (The other parameters are defined as the commercially available PIN diode, MA4AGFCP910.)

The output equal phase point is designed at the focal point (x_f, y_f, z_f). The transmitarray is designed to provide phase compensation, which includes two parts: the incident phase of the illumination wave, and the phase delay from each element to the focal point. Thus, the phase distribution of each element can be calculated according to the equations below:

$$\varphi_{element}(m,n) = -\varphi_{inc}(m,n) + kr_{fmn} + \Delta\varphi, \quad (2)$$

$$r_{fmn} = \sqrt{(x_f - x_{mn})^2 + (y_f - y_{mn})^2 + (z_f - z_{mn})^2}. \quad (3)$$

where φ_{inc} is the measured phase distribution of incident wave, and r_{fmn} is the distance from each element (x_{mn}, y_{mn}, z_{mn}) to the focal point. In these equations, m is chosen as 1, 2, …, 32, and n is chosen as 1, 2. For the 1-bit reconfigurable transmitarray, each element generates only two phase states, 0° and 180°. Hence, a phase

quantization process is applied after Eq. (2). Figure 12 shows the compensated phase distributions for two focal points: (x_f=0mm, y_f=0mm, z_f=80mm) and (x_f=-30mm, y_f=0mm, z_f=80mm).

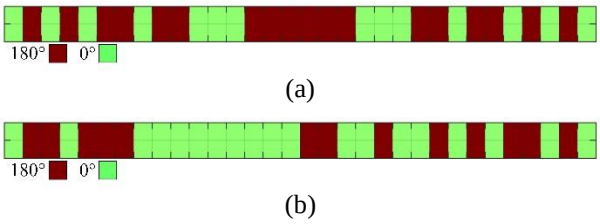

Fig. 12. Phase distribution for the reconfigurable transmitarray: (a) x_f=0mm, y_f=0mm, z_f=80mm; (b) x_f=-30mm, y_f=0mm, z_f=80mm.

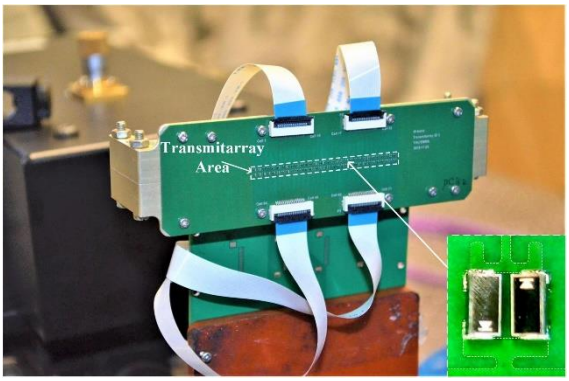

Fig. 13. Prototype of the w-band focus-scanning antenna.

III. EXPERIMENT AND DISCUSSION

A prototype of the 1-bit transmitarray has been fabricated. Prototype of the antenna is shown in Fig. 13. Size of the total antenna structure is 110×34mm^2, containing the total transmitarray of 51.2×3.2mm^2 in the middle. The front layer of arrays, including resonance structures and bias structures, are all printed in the rectangular area. It should be noted that the upper elements and the lower elements are inverted in y-direction for the purpose of easy biasing. Polarity of the diodes are also symmetrically inverted for these two kinds of elements. Thus, ground lines are all combined. The upper bias voltages and lower bias voltages are inverted to generate the same state for upper and lower elements. The bias lines are extended to 4 connectors with 20 pins at upper and lower edges of the transmitarray, and finally connected to a control board and power supply. At the back layer, the transmitarray is also covered by printed metal, except the rectangular slots as designed.

A w-band probe connected with a VDI frequency converter, which is installed on a scanner, is used to measure XY-plane field distribution at the position of focal points at 96.5GHz. Area of the 2-D plane is 174×174mm^2. Measured result of the focal point at broadside is shown in Fig. 14. Detailed comparison of measured result and calculated result along the x-axis is shown in Fig. 15. The measured half power beam width (HPBW) along x-direction is 6mm, compared to the calculated results of 6mm.

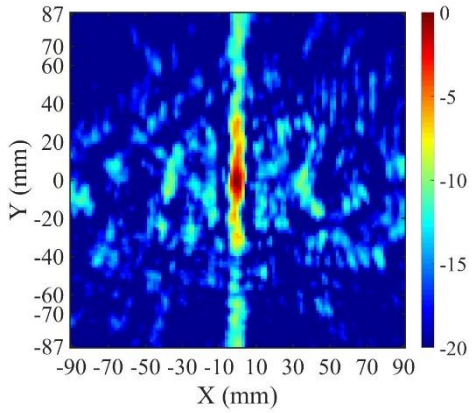

Fig. 14. Measured 2-D result of focal point at x_f=0mm, y_f=0mm, z_f=80mm. (Unit: dB).

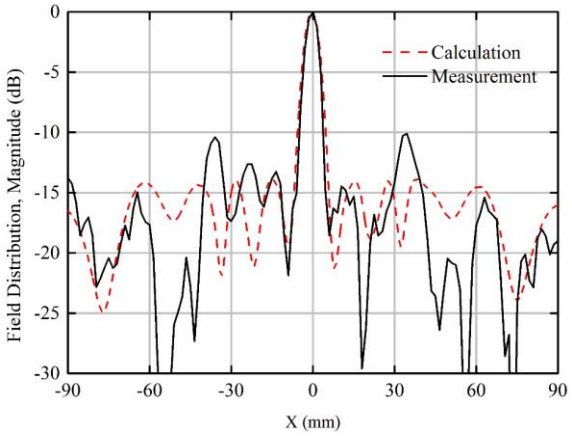

Fig. 15. Comparison between the measured result and the calculated result along x-direction for the focal point at x_f=0mm, y_f=0mm, z_f=80mm.

1-D steered focal points of the reconfigurable transmitarray along x-direction are also measured. Figure 16 shows measured steered focal points from x_f=0mm to x_f=-30mm. The location of measured focal plane keeps the same at z_f=80mm. Measured results of focal points also show that steered focal points keep stable. The location of measured focal point keeps in accordance with the design from x_f=0mm to x_f=-30mm. The half power beam width keeps under 6mm, which is

in accordance with the calculated result. This small HPBW shows promising applications for high-resolution imaging applications.

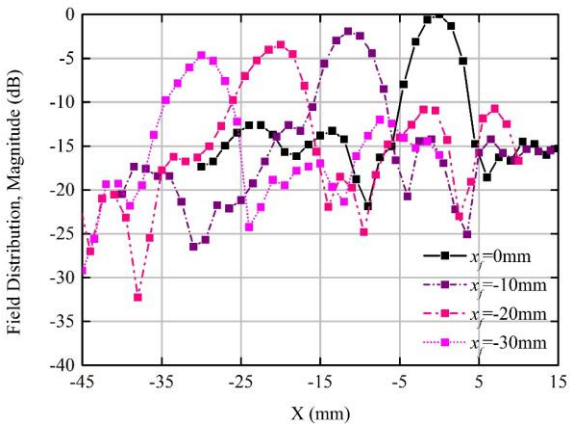

Fig. 16. Magnitude distribution for the 1-D steered focal points along x-direction.

IV. CONCLUSION

A w-band focus-scanning method based on PIN-diode RTA is proposed. The 1-bit phase accommodation is designed for scanning focal points. Based on PIN diode, the beam switching can be conducted in a very short time. Under the switchable states of two PIN diodes, a two-layer symmetrically resonance structure is formed. This design can generate the x-polarization output waves with opposite directions, and guarantee the precise phase shift of 180°. A transmitarray with 32×2 elements is finally fabricated for verification of steerable focal points. Measured results show good agreement with the calculated results. Scanning focal points at x-direction are also measured, which verify the functionality of the RTA design. The proposed method shows notable advantages in weight, size and cost. These features make this antenna suitable for w-band high-resolution fast-speed imaging applications, especially for security checking.

REFERENCES

[1] R. Appleby, "The history of passive millimetre-wave imaging at QinetiQ," in *Proc. of SPIE*, vol. 7117, p. 711702, 2008.

[2] D. M. Sheen, D. L. McMakin, and T. E. Hall, "Combined illumination cylindrical millimeter-wave imaging technique for concealed weapon detection," in *Proc. AeroSense*, pp. 52-60, 2000.

[3] S. V. Hum and J. Perruisseau-Carrier, "Reconfigurable reflectarrays and array lenses for dynamic antenna beam control: A review," *IEEE Trans. Antennas Propag.*, vol. 62, no. 1, pp. 183-198, 2014.

[4] G. Perez-Palomino, P. Baine, R. Dickie, M. Bain, J. A. Encinar, R. Cahill, M. Barba, and G. Toso, "Design and experimental validation of liquid crystal-based reconfigurable reflectarray elements with improved bandwidth in F-band," *IEEE Trans. Antennas Propag.*, vol. 61, no. 4, pp. 1704-1713, 2013.

[5] S. Montori, E. Chiuppesi, P. Farinelli, L. Marcaccioli, R. V. Gatti, and R. Sorrentino, "W-band beam-steerable MEMS-based reflectarray," *Int. J. Microw. Wireless Tech.*, vol. 3, no. 5, pp. 521-532, 2011.

[6] N. Ojaroudi, Y. Ojaroudi, S. Ojaroudi, Y. Ebazadeh, and M. Shirgir, "Small reconfigurable monopole antenna integrated with PIN diodes for multimode wireless communications," *Applied Computational Electromagnetics Society (ACES) Journal*, vol. 29, no. 7, pp. 541-546, 2014.

[7] M. Wang, S. Xu, F. Yang, and M. Li, "Design and measurement of a 1-bit reconfigurable transmitarray with subwavelength H-shaped coupling slot elements," *IEEE Trans. Antennas Propag.*, vol. 67, no. 5, pp. 3500-3504, 2019.

[8] L. Di Palma, A. Clemente, L. Dussopt, R. Sauleau, P. Potier, and P. Pouliguen, "1-Bit reconfigurable unit cell for Ka-band transmitarrays," *IEEE Antennas Wireless Propag. Lett.*, vol. 15, pp. 560-563, 2016.

[9] Https://www.macom.com/products/product-detail/MA4AGFCP910.

[10] X. Pan, F. Yang, S. Xu, and M. Li, "Mode analysis of 1-Bit reflectarray element using p-i-n diode at W-band," in *IEEE Int. Symp. Antennas Propag. Soc.*, San Diego, U.S., pp. 2055-2056, 2017.

[11] A. Khidre, F. Yang, and A. Z. Elsherbeni, "Reconfigurable microstrip antenna with tunable radiation beamwidth," in *IEEE Int. Symp. Antennas Propag. Soc.*, Florida, U.S., pp. 1444-1445, 2013.

Xiaotian Pan received the B.S. degree from Zhengzhou University in 2013, and the M.S. degree from Beihang University in 2016. He is currently pursuing the Ph.D. degree with the Department of Electronic Engineering in Tsinghua University. His current research interests include reconfigurable reflectarray, reconfigurable transmitarray, and the imaging applications.

Fan Yang (Fellow, IEEE) received the B.S. and M.S. degrees from Tsinghua University, Beijing, China, in 1997 and 1999, respectively, and the Ph.D. degree from the University of California at Los Angeles (UCLA) in 2002. From 1994 to 1999, he was a Research Assistant at the State Key Laboratory of Microwave and Digital Communications, Tsinghua University. From 1999 to 2002, he was a Graduate Student Researcher at the Antenna Laboratory, UCLA. From 2002 to 2004, he was a Post-Doctoral Research Engineer and Instructor at the Electrical Engineering Department, UCLA. In 2004, he joined the Electrical Engineering Department, The University of Mississippi, as an Assistant Professor, and was promoted to the post of an Associate Professor in 2009. In 2011, he joined the Electronic Engineering Department, Tsinghua University, as a Professor, and has served as the Director of the Microwave and Antenna Institute since then.

His research interests include antennas, surface electromagnetics, computational electromagnetics, and applied electromagnetic systems. He has published over 300 journal articles and conference papers, six book chapters, and five books. Yang is a fellow of the ACES. He has been a recipient of several prestigious awards and recognitions, including the Young Scientist Award of the 2005 URSI General Assembly and of the 2007 International Symposium on Electromagnetic Theory, the 2008 Junior Faculty Research Award of the University of Mississippi, the 2009 inaugural IEEE Donald G. Dudley Jr. Undergraduate Teaching Award, and the 2011 Recipient of Global Experts Program of China. He was the Technical Program Committee (TPC) Chair of the 2014 IEEE International Symposium on Antennas and Propagation and USNC-URSI Radio Science Meeting. He has served as an Associate Editor for the IEEE Transactions on Antennas and Propagation (2010–2013) and an Associate Editor-in-Chief of the Applied Computational Electromagnetics Society (ACES) Journal (2008–2014). He is also an IEEE APS Distinguished Lecturer (2018–2020).